Geology

Global decline in ocean ventilation, oxygenation, and productivity during the Paleocene-Eocene Thermal Maximum: Implications for the benthic extinction

Arne M.E. Winguth, Ellen Thomas and Cornelia Winguth

Geology published online 23 January 2012;
doi: 10.1130/G32529.1

Notes

Geology, published online on 23 January 2012 as doi:10.1130/G32529.1

Global decline in ocean ventilation, oxygenation, and productivity during the Paleocene-Eocene Thermal Maximum: Implications for the benthic extinction

Arne M.E. Winguth[1], Ellen Thomas[2], and Cornelia Winguth[1]
[1]Department of Earth and Environmental Sciences, University of Texas at Arlington, 500 Yates Street, Arlington, Texas 76019, USA
[2]Department of Geology and Geophysics, Yale University, P.O. Box 208109, New Haven, Connecticut 06520-8109, USA, and Department of Earth and Environmental Sciences, Wesleyan University, Middletown, Connecticut 06459, USA

ABSTRACT

The prominent global warming event at the Paleocene-Eocene boundary (55 Ma), referred to as the Paleocene-Eocene Thermal Maximum (PETM), was characterized by rapid temperature increase and changes in the global carbon cycle in <10,000 yr, and a major extinction of benthic foraminifera. We explore potential causes of this extinction in response to environmental changes linked to a massive carbon injection by comparing sedimentary records with results from a comprehensive climate–carbon cycle model, and infer that an increase in oceanic vertical temperature gradients and stratification led to decreased productivity and oxygen depletion in the deep sea. Globally, productivity diminished particularly in the equatorial zone by weakening of the trades and hence upwelling, leading to a decline in food supply for benthic organisms. In contrast, near the Ross Sea, export of organic matter into the deep sea was enhanced due to increased near-surface mixing related to a positive salinity anomaly caused by a rise in wind-driven vertical mixing, contributing to the depletion of the deep-sea oxygen concentration, combined with a sluggish deep-sea circulation. The extinction of deep-sea benthic foraminifera at the PETM thus was probably caused by multiple environmental changes, including decreased carbonate saturation and ocean acidification, lowered oxygen levels, and a globally reduced food supply, all related to a massive carbon injection.

INTRODUCTION

A prominent global warming or hyperthermal event, referred to as the Paleocene-Eocene Thermal Maximum (PETM), occurred at the Paleocene-Eocene boundary (55 Ma). The PETM was marked by a rapid rise in surface and deep-sea temperature (Kennett and Stott, 1991; Thomas and Shackleton, 1996; Tripati and Elderfield, 2005; Sluijs et al., 2007; Zachos et al., 2008) associated with a major (>3.0‰) negative carbon isotope excursion of controversial origin (e.g., Dickens et al., 1997; McCarren et al., 2008), and shoaling of the carbonate compensation depth (Zachos et al., 2005). The PETM coincided with the most severe extinction of deep-sea benthic foraminifera in the past 100 m.y. (Thomas, 2007) and a large-scale reorganization of planktic organisms, including migration of low-latitude taxa to higher latitudes and rapid evolutionary turnover (e.g., Sluijs et al., 2006; Gibbs et al., 2010).

Plausible causes of the benthic extinction include low oxygen, through lower solubility at the surface by global warming and reduced ocean overturning circulation, through rise in regional oxygen utilization due to enhanced carbon influx in the deep sea by ballasting or marine snow (Armstrong et al., 2002) or by regionally enhanced productivity in marginal basins and along continental margins (Gibbs et al., 2006), and through oxidation of methane released from clathrates (Dickens et al., 1997). Other potentially adverse environmental conditions were an increase in the corrosivity of deep water (Zachos et al., 2005), and a decrease in the food supply through decreased productivity (Thomas et al., 2008).

The analysis of productivity proxies has, however, resulted in conflicting interpretations of productivity changes across the PETM. Productivity might have been either reduced, associated with a nutrient-depleted euphotic zone (Gibbs et al., 2006), unchanged (Paytan et al., 2007), or increased in response to high nutrient availability (Bains et al., 1999; Stoll and Bains, 2003; Stoll et al., 2007) due to enhanced weathering (Ravizza et al., 2001) and/or sea-level rise (Harding et al., 2011). Estimates of high productivity based on Ba accumulation rates (Bains et al., 1999) have been refuted with the adoption of newer age models (Torfstein et al., 2010). An increase in weathering rates is supported by an increase in extratropical precipitation during the PETM, as inferred from observations (Robert and Kennett, 1994; Brinkhuis et al., 2006; Sluijs et al., 2006) as well as climate modeling (Lunt et al., 2010; Winguth et al., 2010).

In this study, the combined dynamic changes of productivity and oxygen distribution in the intermediate and deep-water masses in response to temperature increase and nutrient availability are assessed by applying a comprehensive climate–carbon cycle model to the PETM and by comparison of the results with the sedimentary record. We hypothesize that the reduced overturning circulation associated with ocean warming and high-latitude freshening of the surface in response to massive carbon injection during the PETM led to changes in the environmental conditions (deep-sea anoxia, warming, and ocean acidification) that triggered the benthic extinction.

MODEL DESCRIPTION AND FORCING

The PETM climate simulations have been carried out with the Community Climate System Model Version 3 (CCSM3; Collins et al., 2006), including an ocean carbon cycle model (Appendix DR1 in the GSA Data Repository[1]) with a spectral horizontal resolution of T31 (~3.75° × 3.75°), and vertically 26 unevenly spaced terrain-following levels in the atmosphere, and a nominal 3° horizontal grid with 25 layers in the vertical coordinate in the ocean. For further details about the model configuration and PETM parameter settings, see Winguth et al. (2010) and Appendix DR1. Three sensitivity experiments have been integrated with improved geography for 2500 yr (one with 4, one with 8, and one with 16 times the preindustrial atmospheric CO_2 level, PAL, of 280 ppmv). The increase from 4× to 16× CO_2 would have been equivalent to a total injection of 6700 Gt C, in line with the concept that massive quantities of ^{13}C-depleted carbon were rapidly released into the climate system during the PETM (Panchuk et al., 2008).

RESULTS

Deep-Sea Circulation

The simulated Pacific circulation in the 4× CO_2 scenario is nearly symmetric about the equator (Fig. 1A), with deep-sea ventilation occurring in the polar regions of the Northern and Southern Hemispheres, in

[1]GSA Data Repository item 2012066, Appendices DR1 (model description) and DR2 (Table DR1), is available online at www.geosociety.org/pubs/ft2012.htm, or on request from editing@geosociety.org or Documents Secretary, GSA, P.O. Box 9140, Boulder, CO 80301, USA.

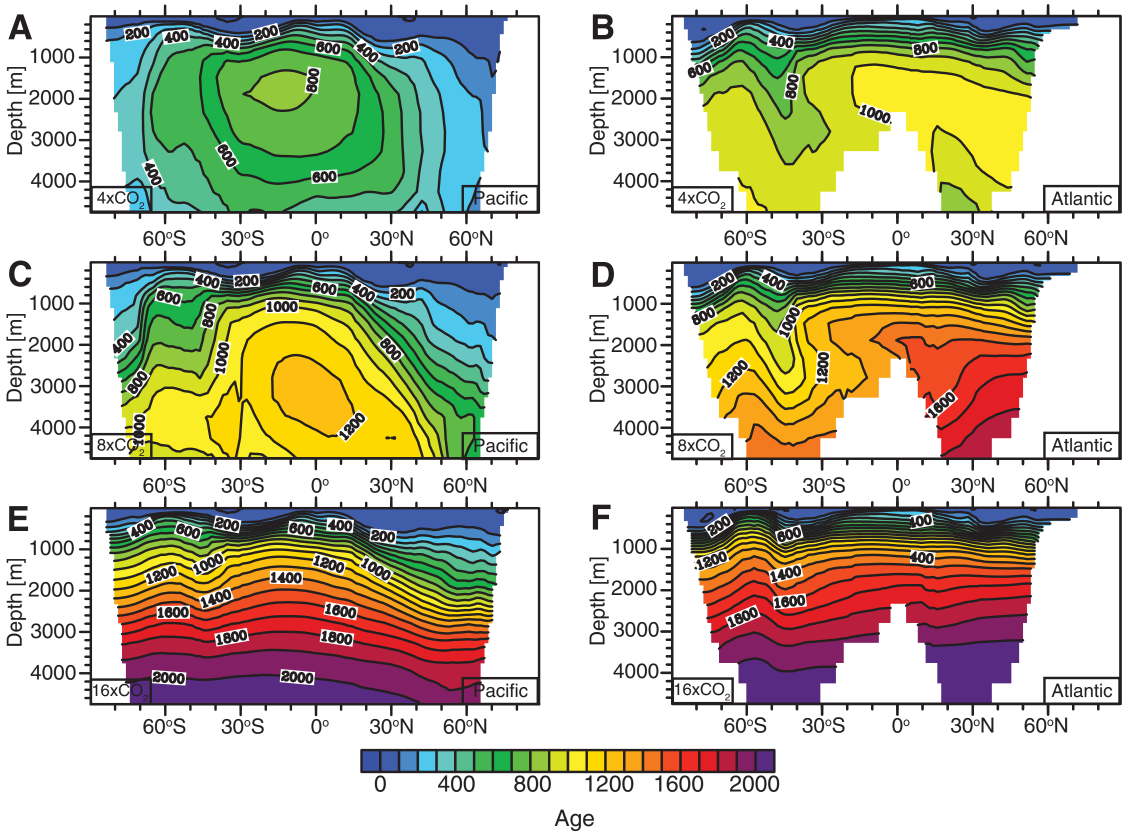

Figure 1. Sections of idealized age of water masses for Paleocene-Eocene Thermal Maximum (100 yr zonal mean). A: 4× CO_2 Pacific. B: 4× CO_2 Atlantic. C: 8× CO_2 Pacific. D: 8× CO_2 Atlantic. E: 16× CO_2 Pacific. F: 16× CO_2 Atlantic.

agreement with Nd isotope data indicating bimodal ventilation (Thomas et al., 2008). In comparison to the present day, the Atlantic circulation was reversed in the 4× CO_2 scenario (Fig. 1B): a northward-directed deep-sea circulation of 4 Sv occurred, with a source of deep-water formation in the South Atlantic. The deep-sea circulation changed considerably with a carbon injection of 2200 Gt C into the atmosphere equivalent to an increase of the CO_2 radiative forcing to ~8× CO_2 (Fig. 1C); the amount of deep-water formation from the southern polar source and in particular from the northern Pacific source was reduced, hence the Pacific deep sea became less ventilated. The Atlantic deep-sea circulation in the 8× CO_2 scenario (Fig. 1D) remained reversed, in contrast with the abrupt shift in the deep-sea circulation during the PETM to a North Atlantic deep-water source based on benthic carbon isotope records (Nunes and Norris, 2006). Southeast Atlantic benthic carbon isotope records suggest that dissolution may have affected the stable isotope records (McCarren et al., 2008), in agreement with the inferred $[CO_3^{2-}]$ gradients in the deep sea (Zeebe and Zachos, 2007). With a total carbon pulse of 6700 Gt C (Panchuk et al., 2008) or increase of atmospheric CO_2 to ~16× PAL, a rise in high-latitude surface temperatures and decrease in salinity by enhanced precipitation resulted in an increase in stratification, leading to a decline in ventilation of the Atlantic and Pacific (Figs. 1E and 1F).

Export Production and Oxygen Distribution

A severe turnover occurred in planktonic marine faunas and floras during the PETM (Sluijs et al., 2007; Gibbs et al., 2010), and shelf productivity increased in contrast with a decrease in open ocean productivity (Appendix DR2). Hypotheses related to the influence of changes in open-ocean productivity on the extinction of benthic foraminifera are controversial (see Thomas, 2007); a long-lived decrease in productivity may have led to the starvation of benthic organisms, whereas an increase in productivity could have caused low-oxygen, inhospitable conditions in the deep sea. In addition, the increased carbon corrosivity may have affected calcareous foraminifera. Noncalcareous agglutinated benthic foraminifera would not have been affected by carbonate corrosivity, but also underwent extinction (Kaminski and Gradstein, 2005).

In order to quantify the causes of the benthic extinction, we compared the two carbon-pulse scenarios (8× CO_2 and 16× CO_2) with the baseline 4× CO_2 scenario. For the 4× CO_2 scenario (Fig. 2A), high productivity is simulated in the equatorial and coastal upwelling zones and in high latitudes due to a rigorous overturning circulation. A carbon pulse to 8× CO_2 PAL reduces the export production by ~22% globally, due to increased stratification and reduction of vertical mixing. In the equatorial Pacific, Ekman-induced upwelling and nutrient availability are reduced, due to a weakening of the trade winds in a higher CO_2 world (Fig. 2B). An even larger carbon increase to 16× CO_2 PAL further diminishes the export production by 20% (or 42% relative to 4× CO_2) in response to a drastic increase in stratification (particularly in the northwestern and southernmost Pacific), a remarkable decline of the deep-sea circulation, and weakened equatorial upwelling (Fig. 2C).

In the 4× CO_2 scenario, the main areas of ventilation are located in the high-latitude Pacific, whereas the lowest oxygen concentrations are predicted for the deep southern Atlantic and Indian Oceans (Fig. 3A). With global warming and increased stratification in the 8× CO_2 simulation, oxygen concentration is strongly reduced, particularly in the intermediate to deep South Atlantic and South Pacific. In the 16× CO_2 experiment, oxygen concentration diminishes to <1 mL L^{-1} in the southern oceans by a further increase in stratification and decrease in solubility due to warming.

Planktic foraminifera and calcareous nannofossil assemblages indicate decreased productivity at Pacific Ocean Drilling Program (ODP) Sites 865, 1209, and 1210 (Appendix DR2). Benthic foraminiferal accumulation rates suggested an increased food supply at Site 865, but application of a recent age model points to decreased food combined with decreased oxygenation. Ichnofossil evidence indicates lowered oxygenation during the PETM at New Zealand localities (Nicolo et al., 2010).

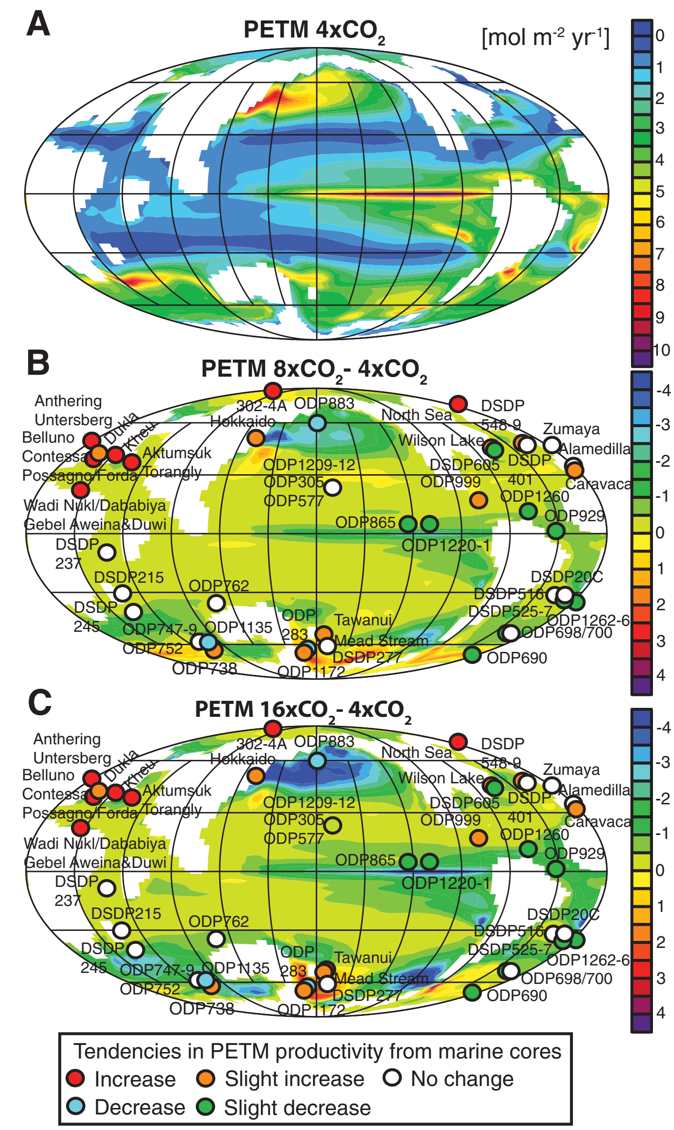

Figure 2. Export production (in mol m⁻² yr⁻¹) for Paleocene-Eocene Thermal Maximum (PETM) simulated with Community Climate System Model Version 3 (Winguth et al., 2010) (100 yr mean) and comparison with productivity tendencies from observations (Appendix DR2; see footnote 1). DSDP—Deep Sea Drilling Project; ODP—Ocean Drilling Program. A: 4× CO_2 scenario. B: Differences 8× CO_2 – 4× CO_2 scenario. C: Differences 16× CO_2 – 4× CO_2 scenario.

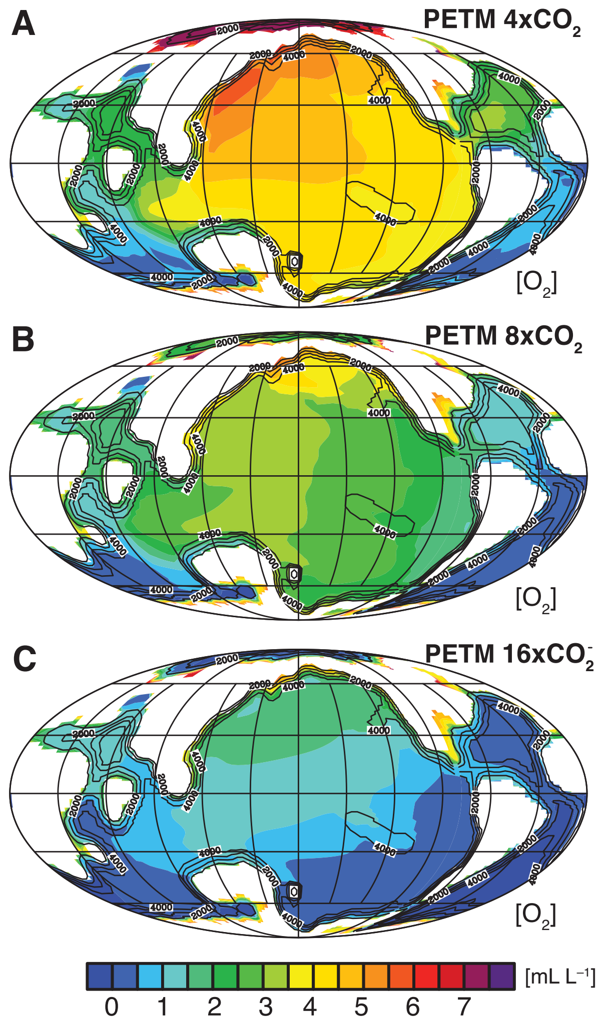

Figure 3. Maps of simulated dissolved oxygen (in mL L⁻¹; 100 yr mean) in bottom layer for Paleocene-Eocene Thermal Maximum (PETM). A: 4× CO_2. B: 8× CO_2. C: 16× CO_2.

In the Southern Ocean near ODP Site 690, simulated productivity does not change significantly during increasing atmospheric CO_2, in agreement with nannoplankton productivity estimates (Gibbs et al., 2010). Benthic foraminiferal evidence from Sites 689 and 690 can be seen as indicative of a decreased food supply combined with lowered oxygenation (Thomas, 1998). In the southeastern Atlantic, geochemical evidence indicates a downward expansion of the oxygen-minimum zone to below 1500 m (Chun et al., 2010), but persistent oxygenation below 3500 m, in agreement with foraminiferal evidence. The severe drop in global productivity as well as the lowered oxygenation and oceanic acidification may have affected the benthic foraminiferal assemblages, especially because at higher temperatures metabolic rates increase, leading to enhanced needs for food (e.g., Thomas, 2007). The rapid rise of atmospheric CO_2 levels and associated climatic changes with enhanced extratropical precipitation in nearshore areas, particularly in the circum-Tethys (Winguth et al., 2010), led to erosion of organic deposits and their transport to nearshore regions, thus contributing to enhanced fertilization (Ravizza et al., 2001) and coastal productivity (Appendix DR2). CCSM3 does not resolve the shelf areas, and nutrient inventories are kept constant, which can explain the model-data biases in nearshore regions.

CONCLUSIONS

The modeling results suggest that wide regions of the South Atlantic Ocean may have become depleted in oxygen during the PETM as a result of a substantial reduction of the deep-sea ventilation (in agreement with Chun et al., 2010), while low-latitude Pacific deep waters underwent less severe depletion. A reduction of the global export production in the open ocean of as much as 42% (difference between 16× CO_2 and 4× CO_2 scenarios) is inferred from our simulations, because diminished equatorial upwelling and reduced deep-water formation in the North Pacific led to enhanced vertical nutrient and oxygen gradients. This study also implies that nutrient supply by erosion must have been enhanced significantly in order to be consistent with increased productivity in coastal regions (Fig. 2; Appendix DR2).

The combined effects of higher bottom-water temperature, reduced deep-sea circulation, changes in surface-water productivity, lower dissolved O_2 concentration, and more corrosive waters in response to the massive carbon injection (Ridgwell and Schmidt, 2010) produced adverse environmental conditions for benthic foraminifera.

The recovery phase after the PETM was probably characterized by a rapid regrowth of terrestrial and marine organic inventories (Bowen and Zachos, 2010). A positive feedback between a cooler climate, an ocean circulation that became more vigorous due to intensification of the wind-driven upwelling and enhanced high-latitude mixing, and the resulting increased global productivity could eventually have accelerated the draw-down of the atmospheric CO_2.

ACKNOWLEDGMENTS

The work was funded by National Science Foundation (NSF) grants EAR-0628336 (Winguth) and OCE-0902959 (Thomas), and simulations were carried out on National Center for Atmospheric Research computers.

REFERENCES CITED

Armstrong, R.A., Lee, C., Hedges, J.I., Honjo, S., and Wakeham, S.G., 2002, A new, mechanistic model for organic carbon fluxes in the ocean based on the quantitative association of POC with ballast minerals: Deep-Sea Research, v. 49, p. 219–236.

Bains, S.R., Corfield, R., and Norris, R.D., 1999, Mechanisms of climate warming at the end of the Paleocene: Science, v. 285, p. 724–727, doi:10.1126/science.285.5428.724.

Bowen, G.J., and Zachos, J.C., 2010, Rapid carbon sequestration at termination of the Palaeocene-Eocene Thermal Maximum: Nature Geoscience, v. 3, p. 866–869, doi:10.1038/ngeo1014.

Brinkhuis, H., and 21 others, and the Expedition 302 Scientists, 2006, Episodic fresh surface waters in the Eocene Arctic Ocean: Nature, v. 441, p. 606–609, doi:10.1038/nature04692.

Chun, C.O.J., Delaney, M.L., and Zachos, J.C., 2010, Paleoredox changes across the Paleocene-Eocene thermal maximum, Walvis Ridge (ODP Sites 1262, 1263, and 1266): Evidence from Mn and U enrichment factors: Paleoceanography, v. 25, PA4202, doi:10.1029/2009PA001861.

Collins, W.D., and 14 others, 2006, The Community Climate System Model Version 3 (CCSM3): Journal of Climate, v. 19, p. 2122–2143, doi:10.1175/JCLI3761.1.

Dickens, G.R., Castillo, M.M., and Walker, J.C.G., 1997, A blast of gas in the latest Paleocene: Simulating first-order effects of massive dissociation of methane hydrate: Geology, v. 25, p. 259–262, doi:10.1130/0091-7613(1997)025<0259:ABOGIT>2.3.CO;2.

Gibbs, S.J., Bralower, T.J., Bown, P.R., Zachos, J.C., and Bybell, L.M., 2006, Shelf and open ocean calcareous phytoplankton assemblages across the Paleocene-Eocene Thermal Maximum: Implications for global productivity gradients: Geology, v. 34, p. 233–236, doi:10.1130/G22381.1.

Gibbs, S.J., Stoll, H.M., Bowen, P.R., and Bralower, T.J., 2010, Ocean acidification and surface water carbonate production across the Paleocene–Eocene thermal maximum: Earth and Planetary Science Letters, v. 295, p. 583–592, doi:10.1016/j.epsl.2010.04.044.

Harding, I.C., Charles, A.J., Marshall, J.E.A., Pälike, H., Roberts, A.P., Wilson, P.A., Jarvis, E., Thorne, R., Morris, E., Moremon, R., Pearce, R.B., and Akbari, S., 2011, Sea-level and salinity fluctuations during the Paleocene–Eocene thermal maximum in Arctic Spitsbergen: Earth and Planetary Science Letters, v. 303, p. 97–107, doi:10.1016/j.epsl.2010.12.043.

Kaminski, M.A., and Gradstein, F., 2005, Atlas of Paleogene cosmopolitan deep-water agglutinated foraminifera: Grzybowski Foundation Special Publication 10, 547 p.

Kennett, J.P., and Stott, L.D., 1991, Abrupt deep-sea warming, paleoceanographic changes and benthic extinctions at the end of the Paleocene: Nature, v. 353, p. 225–229, doi:10.1038/353225a0.

Lunt, D.J., Valdes, P.J., Jones, T.D., Ridgwell, A., Haywood, A.M., Schmidt, D.N., Marsh, R., and Maslin, M., 2010, CO_2-driven ocean circulation changes as an amplifier of Paleocene-Eocene thermal maximum hydrate destabilization: Geology, v. 38, p. 875–878, doi:10.1130/G31184.1.

McCarren, H., Thomas, E., Hasegawa, T., Roehl, U., and Zachos, J.C., 2008, Depth-dependency of the Paleocene-Eocene carbon isotope excursion: Paired benthic and terrestrial biomarker records (ODP Leg 208, Walvis Ridge): Geochemistry Geophysics Geosystems, v. 9, Q10008, doi:10.1029/2008GC002116.

Nicolo, M.J., Dickens, G.R., and Hollis, C.J., 2010, South Pacific intermediate water oxygen depletion at the onset of the Paleocene-Eocene thermal maximum as depicted in New Zealand margin sections: Paleoceanography, v. 25, PA4210, doi:10.1029/2009PA001904.

Nunes, F., and Norris, R.D., 2006, Abrupt reversal in ocean overturning during the Paleocene/Eocene warm period: Nature, v. 439, p. 60–63, doi:10.1038/nature04386.

Panchuk, K., Ridgwell, A., and Kump, L.R., 2008, The sedimentary response to Paleocene-Eocene Thermal Maximum carbon release: A model-data comparison: Geology, v. 36, p. 315–318, doi:10.1130/G24474A.1.

Paytan, A., Averyt, K., Faul, K., Gray, E., and Thomas, E., 2007, Barite accumulation, ocean productivity, and Sr/Ba in barite across the Paleocene–Eocene Thermal Maximum: Geology, v. 35, p. 1139–1142, doi:10.1130/G24162A.1.

Ravizza, G., Norris, R.N., Blusztajn, J., and Aubry, M.-P., 2001, An osmium isotope excursion associated with the late Paleocene thermal maximum: Evidence of intensified chemical weathering: Paleoceanography, v. 16, p. 155–163, doi:10.1029/2000PA000541.

Ridgwell, A., and Schmidt, D., 2010, Past constraints on the vulnerability of marine calcifiers to massive carbon dioxide release: Nature Geoscience, v. 3, p. 196–200, doi:10.1038/ngeo755.

Robert, C., and Kennett, J.P., 1994, Antarctic subtropical humid episode at the Paleocene-Eocene boundary: Clay-mineral evidence: Geology, v. 22, p. 211–214, doi:10.1130/0091-7613(1994)022<0211:ASHEAT>2.3.CO;2.

Sluijs, A., and 14 others, and the Expedition 302 Scientists, 2006, Subtropical Arctic Ocean temperatures during the Paleocene/Eocene thermal maximum: Nature, v. 441, p. 610–613, doi:10.1038/nature04668.

Sluijs, A., Brinkhuis, H., Schouten, S., Bohaty, S.M., John, C.M., Zachos, J.C., Reichart, G.-J., Sinninghe Damsté, J.S., Crouch, E.M., and Dickens, G.R., 2007, Environmental precursors to rapid light carbon injection at the Palaeocene/Eocene boundary: Nature, v. 450, p. 1218–1221, doi:10.1038/nature06400.

Stoll, H.M., and Bains, S., 2003, Coccolith Sr/Ca records of productivity during the Paleocene-Eocene Thermal Maximum from the Weddell Sea: Paleoceanography, v. 18, 1049, doi:10.1029/2002PA000875.

Stoll, H.M., Shimizu, N., Ziveri, P., and Archer, D., 2007, Coccolithophore productivity response to greenhouse event of the Paleocene-Eocene Thermal Maximum: Earth and Planetary Science Letters, v. 258, p. 192–206, doi:10.1016/j.epsl.2007.03.037.

Thomas, D., Lyle, M., Moore, T.C., Jr., and Rea, D.K., 2008, Paleogene deep-water mass composition of the tropical Pacific and implications for thermohaline circulation in a greenhouse world: Geochemistry Geophysics Geosystems, v. 9, p. 1–13, doi:10.1029/2007GC001748.

Thomas, E., 1998, The biogeography of the late Paleocene benthic foraminiferal extinction, *in* Aubry, M.-P., et al., eds., Late Paleocene–early Eocene biotic and climatic events in the marine and terrestrial records: New York, Columbia University Press, p. 214–243.

Thomas, E., 2007, Cenozoic mass extinctions in the deep sea; what disturbs the largest habitat on Earth?, *in* Monechi, S., et al., eds., Large ecosystem perturbations: Causes and consequences: Geological Society of America Special Paper 424, p. 1–24, doi:10.1130/2007.2424(01).

Thomas, E., and Shackleton, N.J., 1996, The Palaeocene-Eocene benthic foraminiferal extinction and stable isotope anomalies, *in* Knox, R.W.O., et al., eds., Correlation of the early Paleogene in northwest Europe: Geological Society of London Special Publication 101, p. 401–441, doi:10.1144/GSL.SP.1996.101.01.20.

Torfstein, A., Winckler, G., and Tripati, A., 2010, Productivity feedback did not terminate the Paleocene-Eocene Thermal Maximum (PETM): Climate of the Past, v. 6, p. 265–272, doi:10.5194/cp-6-265-2010.

Tripati, A., and Elderfield, H., 2005, Deep-sea temperature and circulation changes at the Paleocene-Eocene Thermal Maximum: Science, v. 308, p. 1894–1898, doi:10.1126/science.1109202.

Winguth, A.M.E., Shellito, C., Shields, C., and Winguth, C., 2010, Climate response at the Paleocene-Eocene Thermal Maximum to greenhouse gas forcing—A model study with CCSM3: Journal of Climate, v. 23, p. 2562–2584, doi:10.1175/2009JCLI3113.1.

Zachos, J.C., Roehl, U., Schellenberg, S.A., Sluijs, A., Hodell, D.A., Kelly, D.C., Thomas, E., Nicolo, M., Raffi, I., Lourens, L.J., McCarren, H., and Kroon, D., 2005, Rapid acidification of the ocean during the Paleocene-Eocene thermal maximum: Science, v. 308, p. 1611–1615, doi:10.1126/science.1109004.

Zachos, J.C., Dickens, G.R., and Zeebe, R.E., 2008, An early Cenozoic perspective on greenhouse warming and carbon cycle dynamics: Nature, v. 451, p. 279–283, doi:10.1038/nature06588.

Zeebe, R.E., and Zachos, J.C., 2007, Reversed deep-sea carbonate ion basin gradient during Paleocene-Eocene Thermal Maximum: Paleoceanography, v. 22, PA3201, doi:10.1029/2006PA001395.

Manuscript received 5 June 2011
Revised manuscript received 11 October 2011
Manuscript accepted 18 October 2011

Printed in USA